Science of the Total Environment 696 (2019) 133954

Contents lists available at ScienceDirect

Science of the Total Environment

journal homepage: www.elsevier.com/locate/scitotenv

The wildfire problem in areas contaminated by the Chernobyl disaster

Alan A. Ager [a,*], Richard Lasko [b], Viktor Myroniuk [c], Sergiy Zibtsev [d], Michelle A. Day [e], Uladzimir Usenia [f], Vadym Bogomolov [g], Ivan Kovalets [h], Cody R. Evers [i]

[a] USDA Forest Service, Missoula Fire Sciences Laboratory, Rocky Mountain Research Station, Forest Service, United States Department of Agriculture, 72510 Coyote Road, Pendleton, OR 97801, USA
[b] USDA Forest Service, National Headquarters, Fire and Aviation (retired), Washington, DC, USA
[c] National University of Life and Environmental Sciences of Ukraine, 15, Geroiv Oborony Street, Kyiv 03041, Ukraine
[d] National University of Life and Environmental Sciences of Ukraine, 15, Geroiv Oborony Street, Kyiv 03041, Ukraine
[e] Oregon State University, College of Forestry, Forest Ecosystems & Society, 321 Richardson Hall, Corvallis, OR 97331, USA
[f] Institute of Forestry, Republic of Belarus, Gomel, 71, Proletarskaya Street, Gomel 246001, Belarus
[g] Ukrainian Research Institute of Forestry and Forest Melioration, Pushkinska street, Kharkiv 03041, Ukraine
[h] Institute of Mathematical Machines and Systems NAS of Ukraine, prosp. Glushkova, 42, Kiev 03187, Ukraine
[i] Portland State University, Department of Environmental Sciences and Management, Portland, OR, USA

HIGHLIGHTS

- Wildfires are of growing concern in Chernobyl contaminated areas.
- Resuspension of radionuclides from wildfires has potential adverse health effects.
- We built a wildfire simulation system to predict risk of fires and resuspension.
- The results revealed hotspots for fire ignitions and resuspension.
- Targeted fuel breaks and ignition prevention could reduce future resuspension.

GRAPHICAL ABSTRACT

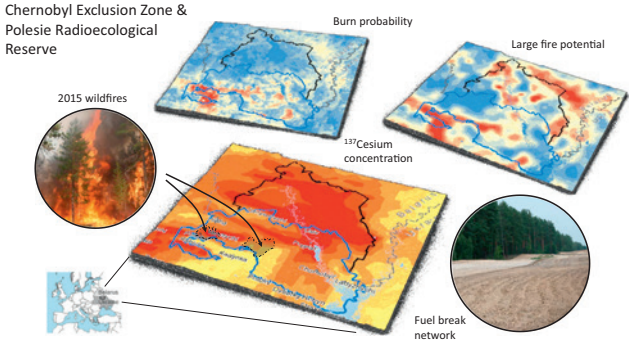

ARTICLE INFO

Article history:
Received 28 March 2019
Received in revised form 15 August 2019
Accepted 15 August 2019
Available online 17 August 2019

Editor: Mae Sexauer Gustin

ABSTRACT

This paper examines the issue of radionuclide resuspension from wildland fires in areas contaminated by the Chernobyl Nuclear Power Plant explosion in 1986. This work originated from a scientific exchange among scientists from the USDA Forest Service, Ukraine and Belarus that was organized to assess science and technology gaps related to wildfire risk management. A wildfire risk modeling system was developed to predict likely hotspots for large fires and where wildfire ignitions will most likely result in significant radionuclide (Cesium, ^{137}Cs) resuspension. The system was also designed to examine the effect of fuel breaks in terms of reducing both burn probability and resuspension. Results showed substantial spatial variation in fire likelihood, size, intensity, and potential resuspension within the contaminated areas. The potential for a large wildfire and resuspension was highest in the Belorussian Polesie Reserve, but the likelihood of such an event was higher in the Ukrainian Chernobyl Exclusion Zone due to a higher predicted probability of ignition. Fuel breaks were most effective in terms of reducing potential resuspension when located near areas that had both high ignition probability and high levels of ^{137}Cs contamination. Simulation outputs highlighted how human activities shape the fire regime and likelihood of a large fire in the contaminated areas. We discuss how the results can be used to develop a fire

* Corresponding author.
E-mail addresses: aager@fs.fed.us (A.A. Ager), victor.myroniuk@nubip.edu.ua (V. Myroniuk), sergiy.zibtsev@nubip.edu.ua (S. Zibtsev), michelle.day@oregonstate.edu (M.A. Day), cevers@pdx.edu (C.R. Evers).

https://doi.org/10.1016/j.scitotenv.2019.133954
0048-9697/Published by Elsevier B.V.

management strategy that integrates ignition prevention, detection, effective suppression response, and fuel breaks. Specifically, the modeling system can now be used to explore a wide range of fire management scenarios for the contaminated areas and contribute to a comprehensive fire management strategy that targets specific drivers of fire by leveraging multiple tools including fire prevention and long-term fuel management. Wildfire-caused emissions of radionuclides in Belarus, Ukraine, and Russia are a socio-ecological problem that will require defragmenting existing risk management systems and leveraging multiple short- and long-term mitigation measures.

Published by Elsevier B.V.

1. Introduction

On April 26, 1986, a routine test of reactor #4 at the Chernobyl Nuclear Power Plant led to an explosion and 10-day fire (Davoine and Bocquet, 2007; Talerko, 2005). About 30 firefighters died during or shortly after from radiation exposure, and >200,000 km^2 of Europe were contaminated with levels of ^{137}Cs above 37 kBq m^{-2}. Over 70% of this area was in the three most affected countries, Belarus, Russia, and Ukraine. The deposition of radionuclides was extremely varied by composition (primarily ^{137}Cs, ^{90}Sr, ^{239}Pu) and amount depending on what part of the reactor was burning where rain intersected contaminated air masses (Yablokov et al., 2009; Chapter 1). Greater than 116,000 people were evacuated in the spring and summer of 1986 from the area surrounding the Chernobyl power plant to non-contaminated areas and >320,000 people were eventually permanently relocated (IAEA, 2006). Two exclusion zones were created around the reactor, one in Ukraine (Chernobyl Exclusion Zone, CEZ; 260,000 ha) and the other in Belarus (Polesie State Radioecological Reserve, PER; 240,000 ha) (Fig. 1) where access is restricted for purposes other than maintaining infrastructure and stabilizing the four nuclear power plants. A wide range of impacts from the radioisotope deposition have been recorded both within and outside of the zones (Brown et al., 2011; Møller et al., 2012). Health effects include numerous diseases and maladies associated with exposure to radioisotopes from the initial explosion and subsequent reactor fire (Yablokov et al., 2009; Chapter 2). Seven-million people are now receiving (or are at least entitled to receive) special allowances, pensions, and health care privileges as a result of the Chernobyl incident (IAEA, 2006).

There are multiple concerns with the increasing incidence of large wildfires in the contaminated areas, including fire fighter exposure to radionuclides, and the long distance transport of resuspended radionuclides in smoke plumes (Evangeliou et al., 2016; Pazukhin et al., 2004). Despite restricted access, human caused fires have been common in both the CEZ and PER, with 1147 ignitions in the CEZ between 1993 and 2013 (Zibtsev et al., 2015). Fires are ignited by vehicles, machinery, electrical transmission lines, arson, and other anthropic events (Dvornik et al., 2017). These fires burn through a mosaic of abandoned forest plantations and agricultural fields and have grown in severity and intensity as a result of accumulating forest and grassland fuels, especially in the large areas covered by Scots pine plantations established during the Soviet era (Fig. 2A; Appendix A, Fig. A1) (Usenia and Yurievich, 2017). Climate anomalies including periods of drought and high temperature have exacerbated the fire problem (Evangeliou et al., 2015). A significant number of fires are ignited in agricultural areas surrounding the CEZ that spread into the reserve. Two human caused wildfire events in April and August of 2015 burned 14,939-ha, one of which originated from a peat ground-fire near the village of Illintsi, and then spread into the CEZ toward the vicinity of the Buriakovka radioactive waste disposal point. Wind and limited accessibility by firefighting equipment contributed to delayed containment of both fires. Firefighters engaged in fire suppression actions are exposed to radionuclides through direct contact and smoke inhalation (Chakrabarty et al., 2006; Kashparov et al., 2015). The secondary exposure to humans from radionuclide particles transported in smoke is a difficult problem to assess and is influenced by many factors: distance, wildfire intensity, duration and size, and characteristics of the smoke plume (Brown et al., 2011).

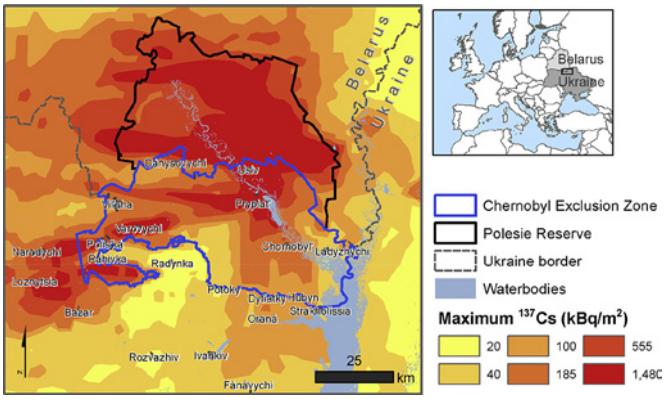

Fig. 1. Map of the study area showing ^{137}Cesium (Cs) deposition levels from the 1986 Chernobyl reactor explosion in Ukraine, Russia, and Belarus (De Cort et al., 1998). Map extent represents the assessment study area with the Chernobyl Exclusion Zone substudy area used for fuel break simulations shown in Fig. 6. The data represent contamination in 1986.

The growing wildfire problem led to a collaborative effort between Ukrainian Government ministries and the United States Forest Service (Lasko, 2016) to develop strategies for improving fire suppression capabilities, increasing firefighter safety by providing respiratory protection and other protective equipment, and identifying fuel management mitigation activities (Lasko, 2011). These early studies also pointed to the need for wildfire risk maps to identify areas of concern for firefighters, and to implement strategic fuel breaks and other long-term forest management strategies. Prior research on the wildfires in contaminated areas included impact assessments under scenarios where the entire CEZ burned in a single fire event (Evangeliou et al., 2014; Hohl et al., 2012). In the Hohl et al. (2012) study, five exposure pathways were examined: 1) external irradiation caused by immersion in a radioactive cloud during plume passage, 2) inhalation of radionuclides during plume passage, 3) external irradiation caused by deposited radionuclides on soil during the year following a wildfire, 4) ingestion of radionuclides in contaminated food during the first years after a wildfire, and 5) inhalation of resuspended radionuclides during the first year following a wildfire. Hohl et al. (2012) concluded that the dosage to people living and working in the CEZ would exceed acceptable levels, but doses to populations further than 30 km from the release point would not require evacuation. Ingestion doses to children (1-y) and older adults would exceed acceptable levels, but would not result in government actions to restrict intakes of contaminated vegetables, meat and milk. In a later study by Evangeliou et al. (2015) wildfires within the CEZ in 2002, 2008 and 2010 were estimated to cumulatively redistribute an estimated 8% of the total ^{137}Cs deposited in the 1986 disaster and predicted to result in significant health effects.

Reconciling these and other studies to assess the potential health effects from wildfires in the contaminated areas is a complex problem owing to fire physics, combustion processes, radionuclide resuspension and transport, and the climate uncertainty associated with extreme wildfire events. In the near term, more detailed analyses are warranted

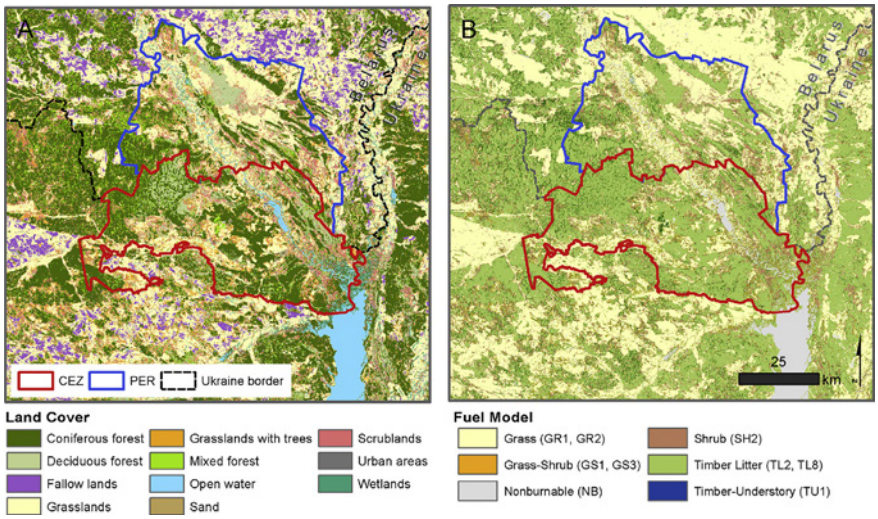

Fig. 2. A) Major vegetation types and boundaries for the Chernobyl Exclusion Zone (CEZ) in Ukraine, and the Polesie Radioecological Reserve (PER) in Belarus. The study area boundary was expanded beyond the contaminated areas to capture wildfire exchange with adjacent lands where field burning and other activities are conducted that provide potential ignition sources. B) Fuel model assignments used in the wildfire simulation. Fuel models were according to Scott and Burgan (2005) and were estimated from a combination of remote sensing data and field observations. See Methods section for additional details.

to describe and map highly likely future fire events to help inform ongoing efforts by government institutions to improve wildfire management strategies (Zibtsev et al., 2015). For instance, prior fire studies lack spatially explicit information on potential wildfire likelihood and impacts that are key inputs into spatially explicit risk abatement strategies (Ager et al., 2015; Miller and Ager, 2013). In this paper we describe the application of a fine scale wildfire simulation system to map where wildfires are most likely to ignite, spread, and resuspend radionuclides. The system incorporates spatial data on ignition likelihood, fuel loads, and ^{137}Cs deposition to simulate fire events and resulting resuspension. In contrast to prior studies that assumed that the entire exclusion zone burned in one or more catastrophic fires (Evangeliou et al., 2014; Hohl et al., 2012), this analysis was conducted at a finer scale and calibrated with local data. We discuss how the modeling framework and results of our assessment can be used to improve fire management strategies by linking specific drivers of high impact events with multiple management tools including ignition prevention, presuppression planning, suppression, and fuel management to minimize future wildfire activity within contaminated areas.

2. Methods

2.1. Study area

The 1.278 10^6-ha study area included the Polesie Radioecological Reserve in Belarus (PER) and the Chernobyl Exclusion Zone (CEZ) in Ukraine (Fig. 1). Extending the study area beyond the boundaries of the reserves allowed us to model and measure the effect of fires started outside the CEZ and PER. In Belarus, the PER is staffed to monitor radioactivity in the reserve and provide management recommendations to the Department for Mitigation of Consequences of the Catastrophe at the Chernobyl NPP of the Ministry of Emergency Situations (DMCCC) (Usenia, 2002; Usenia and Yurievich, 2017). In Ukraine, management of the CEZ is under the control of the State Agency of Ukraine on Exclusion Zone Management.

About 65% of the study area is forested (7663 km^2), composed of plantations of Scots pine (*Pinus sylvestris*, 5207 km^2) and mixed broadleaf stands of oak (*Quercus robur*), birch (*Betula pendula*), aspen (*Populus tremula*), and alder (*Alnus glutinosa*), the latter covering ~2456 km^2 (Fig. 2A). The rest of the study area is abandoned agricultural fields now vegetated with forage grasses that are transitioning into mixed conifer-hardwood forests. Deciduous forests are generally found in the bottomlands and wetter sites.

2.2. Fire simulation model

We used FConstMTT (Brittain, 2017), a command line version of FlamMap that models fire spread with the Minimum Travel Time (MTT) (Finney, 2002) algorithm. This program is part of a larger family of fire simulation models that are widely used for tactical and strategic planning (Alcasena et al., 2016; Noonan-Wright et al., 2011; Palaiologou et al., 2018; Salis et al., 2013). FConstMTT uses as inputs data on fuels, fire weather (wind speed, wind direction), fuel moisture, and spatial ignition probability. These data sources are described individually below.

2.2.1. Fuels data

Inputs for the wildfire simulations required maps of surface and canopy fuels. Surface fuel model maps (Scott and Burgan, 2005) were developed for the study area using Landsat-classification of land cover (Fig. 2B; Appendix A, Table A1) to describe the primary carrier of fire (grass, shrubs, litter). We identified and mapped 11 land cover classes (Fig. 2A) and then assigned a surface fuel model (Fig. 2B) and associated fuel load, fuel type and potential fire behavior. A training dataset was generated using a stratified random sampling frame using recommendations from Olofsson et al. (2014). The Hansen et al. (2013) Global Forest Change (GFC) dataset was used for stratification of the study area into four strata: two stable (forested and non-forested areas) and two change classes (forest loss and forest gain). The sample size was calculated proportionally to strata areas to provide at least 50 samples to characterize each stratum. The distribution of samples by GFC strata was as follows: non-forested area – 450, forested area – 416, forest loss – 50, forest gain – 50. All samples were visually interpreted using the Collect Earth plugin for Google Earth (Bey et al., 2016). The assigned classes are presented in an error matrix (Appendix A, Table A2).

Nearly cloud-free Landsat 8 OLI top of atmosphere (TOA) reflectance images were used for the land cover classification. First we selected 2016 Landsat images having cloud coverage < 5%. Next, clouds were masked if the cloud-likelihood score exceeded 10%. The processing of images was performed by a cloud scoring algorithm in Google Earth Engine (GEE) (Gorelick et al., 2017) using a combination of brightness, temperature and Normalized Snow Index (NDSI). To increase accuracy of the classification we applied a phenology-oriented approach using

four seasonal cloud-free Landsat mosaics as described in Hansen et al. (2010): annual, summer, autumn, April–October. The April–October mosaic addresses the leaf-on period in Ukraine and improves discrimination between woody and herbaceous types of vegetation. The compositing approach used criteria based on per-pixel analysis and selection from multiple cloud-free observations of the same pixel. If several such pixels exist in a compositing period, the observation with the maximum Normalized Difference Vegetation Index (NDVI) was selected (Hansen et al., 2014). For annual, summer and autumn mosaics, the list of predictor variables included TOA reflectance of visible and infrared bands (Band 4 – Band 7), NDVI and bands of Tasseled-Cap Transformation (TCT).

TCT bands were derived following the procedures of Baig et al. (2014) where the original Landsat 8 OLI bands were converted into images that represented brightness, greenness, and wetness. To capture seasonal changes in vegetation, the predictor variables for the April–October mosaic were extracted using statistical rules as follows: minimum and maximum values, 1st, 3rd quartiles and median of TOA reflectance for selected spectral bands (Band 4–Band 7) and NDVI. We also incorporated geographical position data (i.e., latitude and longitude) as ancillary non-spectral covariates. A Random Forest (RF) classifier (Breiman, 2001) was used in GEE, both to classify imagery by land cover categories defined during visual image interpretation and to assess accuracy. RF is a nonparametric ensemble learning approach which uses bagging or bootstrap aggregation to produce unbiased estimates of classification error (out-of-bag, (OOB) error). The overall accuracy of the classification estimated by OOB sampling was 95.6%. There was some misclassification between forests and other land cover types where woody vegetation occurs (e.g., shrubland and grasslands with trees). Coniferous and deciduous forests were distinguished with higher accuracy compared to mixed forests.

Given the absence of spatially explicit forest inventory data for the entire study area, we used the Forest Vegetation Simulator (Dixon and Keyser, 2008) to estimate canopy fuels (canopy bulk density (kg m^{-3}), height to live crown (ft), total stand height (ft), canopy cover (%)). We built a regression model using CEZ inventory data as training inputs, and regression analysis to predict values outside the area covered by the training data set. Area burned by two large fires in April and August 2015 were mapped using Landsat 8 OLI time series, and the canopy values for that area was set to 40% based on field data. Canopy Height (CHT) and Canopy Bulk Density (CBD) were mapped for the study area using the RF regression model with the same list of predictor variables used in the land cover classification. The model was fitted using >23,000 forest polygons for which median values of spectral features had been extracted. Canopy Base Height (CBH) was predicted with a nonlinear regression model using the ratio of CBH/CHT as a response function of CC and CHT. Initial simulations generated acceptable fire behavior although CBH required a downward adjustment to 10% of original values in the open Scots pine stands (<50% canopy) to obtain the crown fire activity observed in recent fires. We suspect that the estimation process did not capture the regeneration in many of the open Scots pine stands that serve as ladder fuels that catalyze crown fire behavior. Raster grids for surface and canopy fuels for the simulations were constructed at a 100-m resolution.

2.2.2. Ignition history and probability grid

Existing ignition history data for the contaminated areas are incomplete in terms of spatial coverage and timespan (Kudin, 2014; Zibtsev et al., 2015). The ignition history for CEZ is outdated and some known large fires are missing, while ignition data for the PER are not available in a digital map format. To build a complete data set that captured fires/ignitions within the entire study area (Ukrainian and Belorussian), official statistics maintained at CEZ were used for the years 1993–2016 (State Special Enterprise Picnichna Puscha, 2019), and MODIS (MOD/MYD14) daily data (NASA, 2015) for 2000–2016. In addition, major fire perimeters were mapped manually using Landsat images.

A time series of Landsat imagery for all MODIS hotspots was analyzed to delineate major fires from 2000 to 2016 for the study area. Since fires with a duration of >1 day can appear as multiple hotspots in the MODIS data, we grouped connected ignitions for each day into separate fires and identified centroids for each of them. For each fire event we created cloudless pre-fire and post-fire image composite mosaics. A total of 1680 fires and associated ignition points from the MODIS data were identified and mapped. MODIS was combined with the empirical data (2458 ignitions, Fig. 3) to create a smoothed ignition probability map using a kernel density function in ArcMap with a search radius of 10,000-m (Fig. 4A). The resulting map was sampled in a Monte Carlo process to locate ignitions for the wildfire simulation.

2.2.3. Fire weather and fuel moisture

Wind speed and direction were derived from historical records from the weather station at the Ukrainian State Hydrometeorological Service at Chernobyl city (51.2763° N, 30.2219° E) for the period 1988–2016. Median values of wind gust and wind direction by day-of-year were used over a total of 10,000 days (Appendix A, Table A3). Although we used a constant wind speed and direction for each fire and ignored intraday wind shifts, the resulting perimeters resembled historical events (see Appendix A, Fig. A2). This is because most of the growth for large multiday fires is achieved in relatively few extreme spread events. These extreme events occur under constant wind direction. This is why most historical fire perimeters are ellipsoids or daily ensembles thereof that generate a larger ellipsoid shape. While detailed intraday (e.g., hourly) weather inputs can be used in fire simulation systems (Noonan-Wright et al., 2011), computational limitations prevent their application for large-scale risk-estimation problems, and only provide marginal improvements in the process due to uncertainty. National risk assessments in the US use daily rather than intraday fire weather

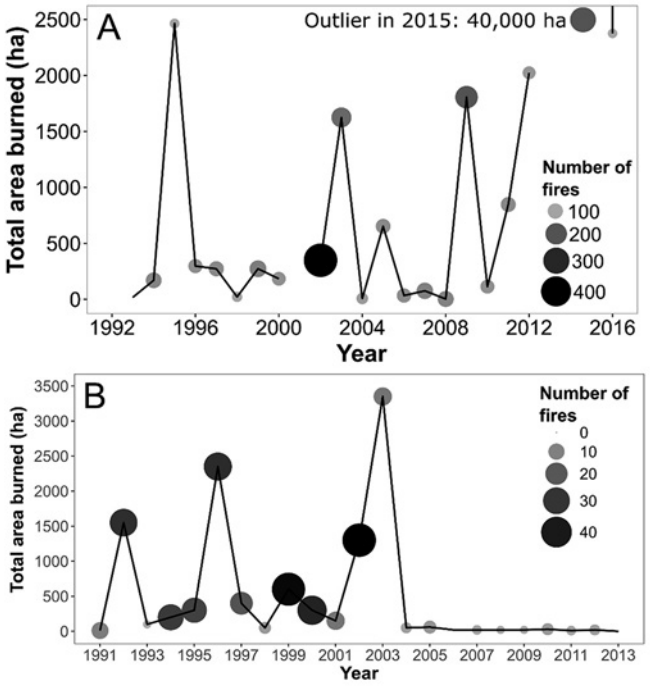

Fig. 3. Area burned and number of fires (A) between 1993 and 2016 in the study area including official statistics and MODIS data and (B) between 1991 and 2013 in the Belorussian Polesie Radioecological Reserve (PER) (Kudin, 2014; spatial attributes not available and therefore not included in simulations). Note the substantial drop in ignitions in the PER after expanded fire suppression measures and access security restrictions were implemented in after extreme fires in 2003 (Usenia et al., 2017). Less than 2% of the fires in the Chernobyl Exclusion Zone were documented as lightning caused, the remaining either unknown or documented as human caused. Leading causes of fire include field burning, machinery from logging operations, hunters and other recreational activities.

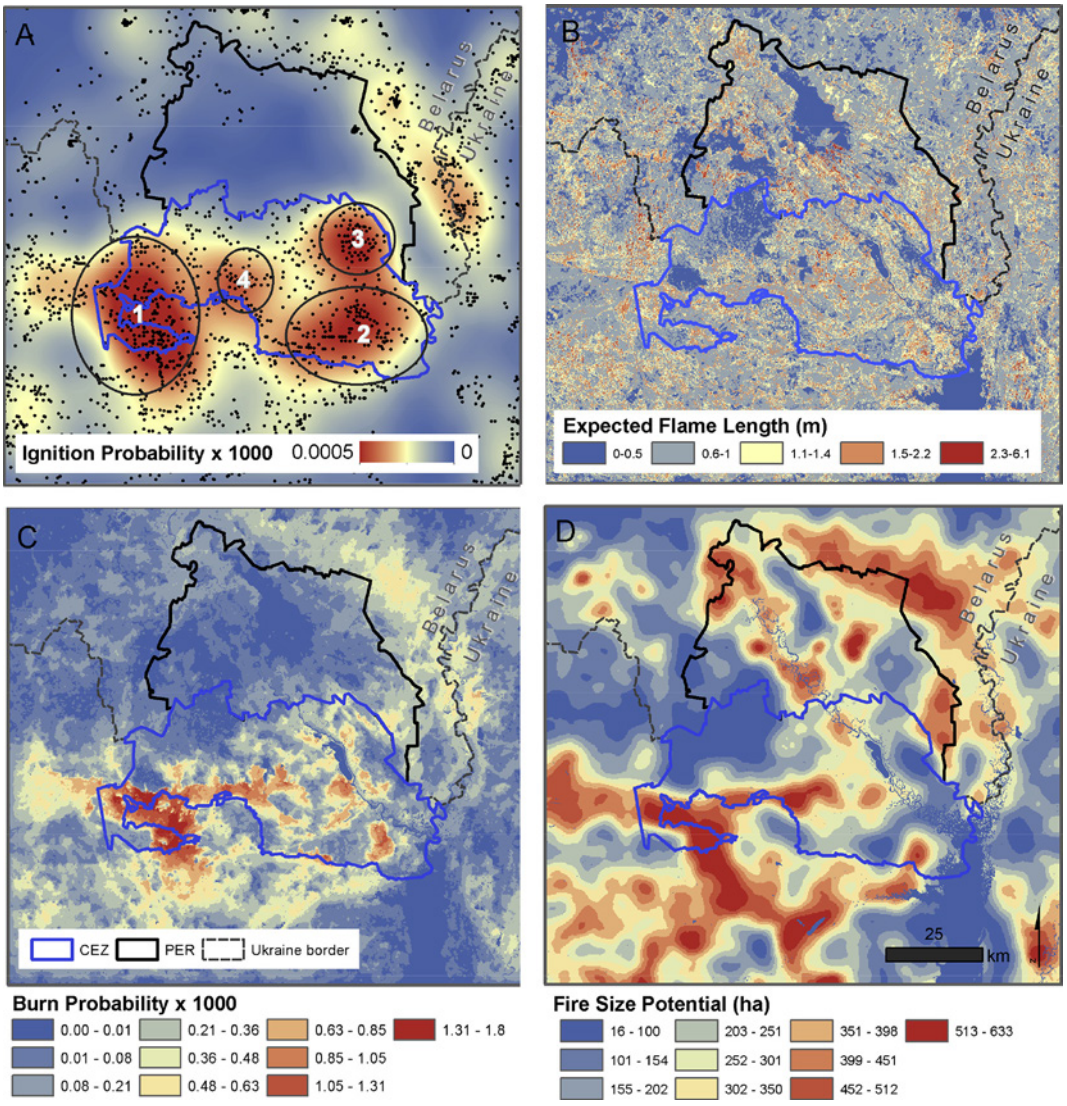

Fig. 4. Ignition probability (A), expected flame length (B), burn probability (C) and fire size potential (D) for the study area predicted from simulation outputs. Historical ignitions (black dots in panel A) are from 1992 to 2016 provided by fire management staff within the Chernobyl Exclusion Zone (CEZ), and obtained from MODIS for the remainder of the study area; resulting ignition probability map was derived from kernel density smoothing. Ignition hot spots are outlined with numbered circles and correspond to the following ignition patterns: 1) international roads, local settlements and their inhabitants, agricultural burning and minimal border security; 2) roads, CEZ staff activity, power lines, forestry, settlers; 3) railroads; and 4) nuclear waste management and other CEZ staff activity, and settlers. Burn probability values represent the likelihood of a fire in a specific location given a single ignition event within the study area. Expected flame length is the frequency weighted flame length for all fires that burned a specific pixel. Hotspots result from a combination of high ignition frequency in historical data and large areas of fuel with high spread rates. Fire size potential generated from simulation outputs. Each simulated ignition point was colored according to the size of the resulting fire. The map shows where ignitions have the highest potential to generate large fires without considering the likelihood of an ignition. PER = Polesie Radioecological Reserve.

conditions in simulations for wildfire risk assessments (Finney et al., 2011).

Fuel moistures were derived from weather data (1995 to 2016) from the Ukrainian Hydrometeorological Center (2016) by estimating the 97th percentile ERC-G fuel moisture content (Nelson, 2000). Fuel moisture was adjusted by vegetation type (conifer, hardwood, grass) and month of year to reflect the phenology of different vegetation types (Appendix A, Tables A3 and A4). Specifically, Behave simulations were used to adjust fuel moistures by month of year to achieve reasonable spread rates and flame lengths on empirical observations of past fires and expert judgement. The calibration replicated the early-season drying of grass fuels and the resulting fast fire spread-rates observed in past grass field fires in the study area and elsewhere in Eastern Europe. The seasonal calibration of the fuel moisture also captured the relatively slow early season spread-rates observed in the conifer and hardwood forests due to the higher fuel moisture conditions and later phenology of understory vegetation. The net result is that we were able to replicate the bimodal fire frequency regime (early season grass fires, later season conifer fires) observed in the central region of Ukraine.

2.2.4. Fire calibration and sensitivity analyses

A number of calibration procedures were performed where historical and simulated fires were compared in terms of spread rates, perimeters, and size distributions. To achieve a size distribution that approximated historical fires (Appendix A, Table A5), 5000 wildfires were simulated using a range of burn periods to build a relationship between fire size and burn period. We then created a frequency distribution of burn periods that coarsely replicated historical fire sizes, a methodology utilized in previous fire modeling studies (Ager et al., 2018). We also qualitatively compared the shape of historical fire perimeters with selected simulated fire events of similar size.

2.2.5. Wildfire scenarios and exposure assessment

We built a set of wildfire scenarios based on daily wind speed and direction, and monthly fuel moistures files (Appendix A, Tables A3 and A4). Scenarios were sampled by FConstMTT with equal probability and used to execute a fire simulation. This Monte Carlo process was repeated to simulate a total of 1.5 10^5 fires. Ignition locations were determined by sampling the spatial ignition probably map developed from historical ignition data. We used one unique weather record per day and twelve fuel model files. The weather data were median values extracted from the CEZ weather database for 1988–2016.

We used fire simulation outputs to describe spatial variation in burn probability and intensity within the study area. The fire simulation system generates a burn-probability grid that is calculated as the count of the number of times a pixel burned divided by the total number of simulated fires. Burn probability represents the likelihood of a pixel burning given one ignition within the study area under the associated simulation parameters. Fire intensity was measured as the average flame length across all fires that burned each pixel. Predicted flame length varies among simulated fires depending on whether the pixel was burned in a flanking, heading, or backing fire (Finney et al., 2011).

2.3. ^{137}Cs spatial distribution

Contamination levels were derived from the Atlas of Caesium-137 Contamination of Europe after the Chernobyl Accident (De Cort et al., 1998), which depicts total deposition of ^{137}Cs contamination (kBq m^{-2}) once the radioactive release from the reactor had stopped (De Cort et al., 1998, pg. 21). Specifically, national deposition maps for Ukraine, Belarus, and western Russia were digitized and projected using ArcGIS and then merged into a single raster grid at 100 m resolution. Note that there are several other published contamination maps (Avramenko et al., 2009; Kashparov et al., 2001) that are all derived from this Atlas, the exception being the plot data of Kashparov et al. (2018) (Fig. 1).

^{137}Cs has high mobility due to its similarity to potassium, and a wide range of factors remove ^{137}Cs from ecosystems, sequester it, or reduce its availability to comubst in a fire (Whicker and Schultz, 1982). For instance, studies of ^{137}Cs migration between 6 km and 30 km from Chernobyl (Shcheglov et al., 2014) showed that 60–87% of the ^{137}Cs had migrated to the mineral soil in the first 15 years after the reactor fire, where it is not available for combustion. To account for both physical decay and removal from the ecosystem by natural processes, we used an effective ^{137}Cs half-life (T_e). There are less than a handful of studies that estimate T_e for ^{137}Cs, and values range widely depending on soil type, season of year and type of vegetation, among other factors (Burger and Lichtscheidl, 2018). We identified the data of Paller et al. (2014) as applicable to Chernobyl due to the similar ecosystem. Paller et al. (2014) studied the T_e of ^{137}Cs around the Savannah River floodplain in the southeastern US where contamination from nuclear facilities has been measured and monitored since 1965. The site is similar to the flood plains of the Prypiat River, although wildfires are rare. The T_e of ^{137}Cs in Savannah River floodplain soil and vegetation was estimated at 17.0 years (95% CI = 14.2–19.9).

We estimated 2018 ^{137}Cs `contamination according to

$$A = A_0 * (0.5)^{DP/Te}$$

where A = 2018 contamination and A_0 = initial or 1986 deposition values, and DP = 32 years since the inventory (1986–2018) mapping, and T_e = 17 years. Note that the effect of prior large wildfires (Zibtsev et al., 2015) was not explicitly factored into T_e primarily because the areas recently burned are not likely to burn again until fuels are sufficient to carry a fire that exceeds suppression capacity.

2.4. Resuspension of radionuclides

Resuspension of radionuclides was estimated by overlaying simulated fire perimeters with maps of ^{137}Cs contamination and assuming a fixed proportion of deposited ^{137}Cs contained within the perimeters would be resuspended from the fire. Specifically, each of the simulated fire perimeters was intersected with gridded data on 2018 ^{137}Cs contamination levels (kBq m^{-2}). Resuspension was then estimated with an emission factor and the total estimated emissions were assigned to the ignition location. These data were smoothed with inverse distance weighting to create a map of the potential ^{137}Cs emissions from a fire ignition location. While a wide range of emissions factors have been reported (Amiro et al., 1996; Evangeliou et al., 2016; Hao et al., 2018; Horrill et al., 1995; Kashparov et al., 2000; Talerko, 2011), most studies report values in the range of 2%–5% (Hao et al., 2018; Kashparov et al., 2000; Talerko, 2011; Yoschenko et al., 2006). Emission-factors within the range of 2–5% have been successfully used for simulations and forecasting of radiological consequences of several real wildfires at distances from about 20 to 200 km from the wildfire (Bogorad et al., 2016; Kovalets et al., 2015; Talerko, 2011). An emission factor of 4–5% is typically used in Ukraine for real-time forecasting of radiological consequences of wildfires in the CEZ (SNRIU, 2019; Talerko et al., 2010). Given these sources, we chose an emission-factor of 5%, recognizing that ^{137}Cs emissions are related to burn severity since the bulk of the contamination within combustible material is in the duff layer (Amiro et al., 1999). Widely different rates of resuspension likely occur within actual wildfires that are a mosaic of fire intensities.

2.5. Fuel break management scenario

We created a fuel break scenario based on existing roads and natural fuel breaks along streams and canals (see Zibtsev et al. (2015); Appendix A, Fig. A3). The vast majority of the planned fuel breaks have never been built, and those that were, have not been maintained (Zibtsev et al., 2015). We simulated the creation of this network by changing the fuels to non-burnable within continuous 200-m wide linear segments. In total, this represented approximately 930-km of fuel breaks for a total area of 186-km^2 (7% of the CEZ). This compares with a total fuel break length of 111-km proposed in the 1990s. Those proposed fuel breaks averaged 20-m in width for a total of 2.76-km^2 (0.1% of the CEZ), as documented in the fire management plan for the CEZ (Zibtsev et al., 2015). We processed the fuel break scenario with the same procedures above, and then quantified the response of the fuel breaks in terms of the change in burn probability, the number of fires that encountered each of the fuel breaks, and the change in fire frequency distribution. For the encounter rate, we discretized the fuel breaks into 2-km segments and intersected them with the simulated fire perimeters to estimate how many fires encountered each fuel break segment. We mapped the encounter rate and examined change between the fuel break scenario versus no treatment. In this way, we were able to quantify the efficiency of individual fuel break segments. We then calculated the difference between the pre- and post-treatment potential emissions for each fire ignition by overlaying the perimeter on the 2018 contamination map. These maps were smoothed with a kernel density procedure and differenced to map the avoided emissions from the fuel break scenario.

3. Results

3.1. Comparison of historical ignition patterns between the PER and CEZ

Our combined ignition data set derived from official fire databases and MODIS reports showed substantial spatiotemporal variation in ignition locations and differences between CEZ and PER (Fig. 4A). In the CEZ, ignitions were clustered near human infrastructure and villages outside the zone and overall were highly non-random. Examination of fire

causes for the CEZ showed <2% were lightning caused, with the bulk of the documented ignitions attributable to humans although 63% of the ignitions in the CEZ data were of unknown origin. Ignitions in the CEZ were 18 times higher than in the PER, and over the period examined (1993–2016 for the CEZ and 2001–2016 for the PER) the annual rate of ignitions was 37 yr^{-1} in the CEZ versus 3 yr^{-1} in the PER. The spike in ignitions in the CEZ around 1995 (Fig. 3A) was attributed to diminished fire management capacity following the breakup of the Soviet Union (Zibtsev et al., 2015). The major drop in ignitions in the PER after 2003 (Fig. 3B) corresponds to the initiation of enhanced security measures in the PER (Usenia et al., 2017).

An important observation on the spatiotemporal patterns of fire activity was the identification of a bimodal wildfire season related to both ignition cause and fuel moistures. Field burning practices by inhabitants on the edge of the CEZ and in resettled areas cause spring grass fires, while fires in forested areas are caused by industrial and other human activities later in the summer when forest fuel moistures decline.

3.2. Fire simulation outputs

Comparison of simulated and historical fire perimeters showed qualitative similarities in terms of shape and size and incidence within the study area (Appendix A, Fig. A2). Comparison of historical fire distribution with simulated fire sizes also showed that the simulations produced fires that mimic historical distributions (Appendix A, Fig. A4). Data show some underestimation of rare, large fire events (e.g. 10,000–13,000 ha) by the simulation model, owing to rare climatic events that are not captured in the median wind speed and average fuel moisture data. However, additional simulations, (e.g., 1 million) could potentially result in these large historical fire events.

Maps of the fire simulation outputs show spatial variation in expected fire behavior as measured by likelihood (burn probability), intensity (expected flame length), and fire size (Fig. 4B–D). Burn probabilities (Fig. 4C) showed relatively high values in the southwest portion of the study area where high ignition frequency in historical data and large areas of fuel with high spread rates are located. Higher values of expected flame length (Fig. 4B) were more diffuse than burn probability, and generally corresponded to areas with Scots pine plantations. Fire size potential, or the propensity of ignitions to generate large wildfires, showed high values in multiple areas within the study area, especially for portions of PER where the burn probability was low (Fig. 4D). The frequency distribution of predicted ^{137}Cs emissions from individual fire events varied from near 0 to a maximum of about 1.72 million kBq (Appendix A, Fig. A5), although predicted emissions for 86% of individual fires were < 8765 kBq. There were 47 fire events where predicted emissions exceeded 2.8 10^5 kBq. The largest emissions event was from a fire that burned 12,684-ha and started in the southern portion of the Polesie reserve.

The emissions potential (Fig. 5A) that is a measure of the propensity of an ignition location to spawn large fires that spread into contaminated areas showed high values in and around the most contaminated areas, especially within the PER. The expected emissions, which factors ignition probability (Fig. 4A) as well as fire size potential (Fig. 4D), showed the highest values in the CEZ (Fig. 5B). Overall, the simulations identified the areas of greatest concern with respect to both the potential and expected fire behavior considering historical ignition frequency, fire intensity, spread rate, and contamination.

3.3. Effect of fuel break network

Effect of the simulated fuel break network on reducing burn probability within the CEZ was generally concentrated where ignition frequency was the highest (Fig. 6). Note that the fuel break simulation experiment was only conducted for the CEZ due to lack of spatial location data for fuel breaks in the Polesie reserve. The change in fire size distributions showed that the fuel break scenario reduced the incidence of larger fires (Fig. 7A). The intercept frequency was used to measure the performance of individual 2 km fuel break segments and showed that a small number of fuel breaks accounted for the majority of the intercept (Fig. 7B). Maps of the intercepts (Fig. 7B) showed intercept frequency was highest in the southwest and southern portions of the CEZ. The effect of the fuel break network on potential and expected

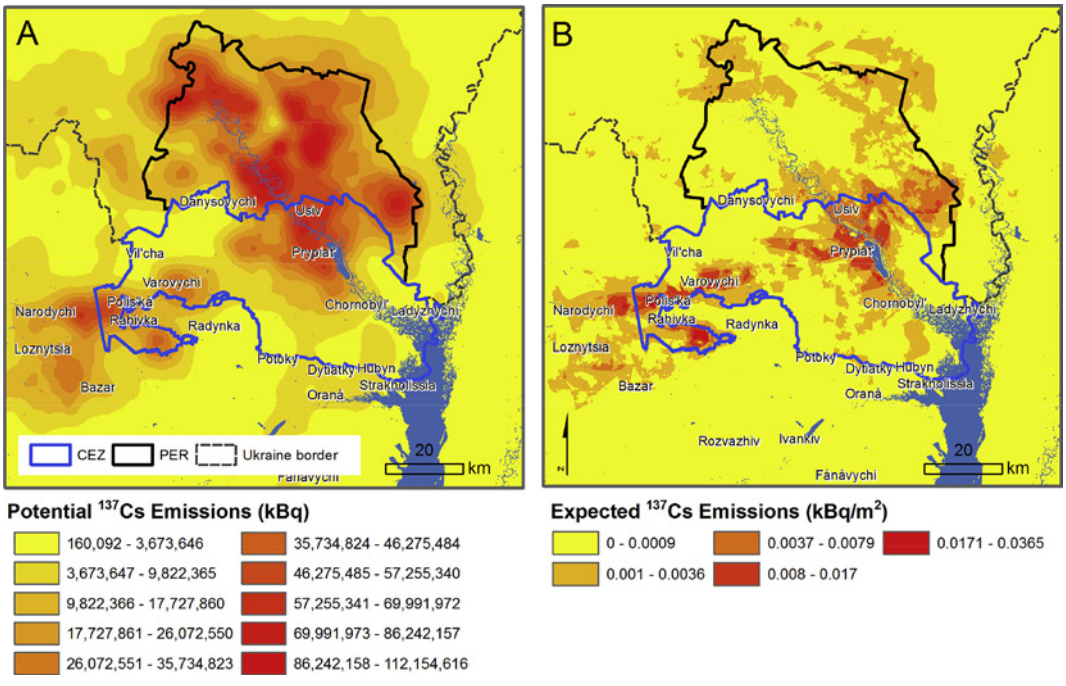

Fig. 5. (A) Potential ^{137}Cesium (Cs) emissions from simulated ignitions and resulting fire. Each simulated ignition point was colored according to the total 2018 ^{137}Cs contamination resuspended within the resulting fire perimeter. The map shows where ignitions have the highest potential to generate large fires that also burn through highly contaminated areas and resuspend ^{137}Cs. (B) Expected ^{137}Cs emissions accounting for historical ignition patterns and burn probability. CEZ = Chernobyl Exclusion Zone, PER = Polesie Radioecological Reserve.

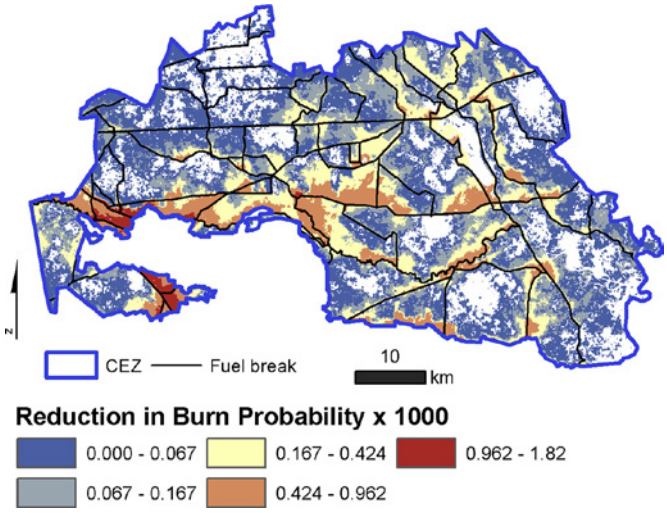

Fig. 6. Effect of fuel breaks on burn probability from wildfire simulations within the Chernobyl Exclusion Zone (CEZ) portion of the study area. Image was generated by simulating wildfires on a landscape where the fuel breaks were considered non-burnable fuels for 200-m in width.

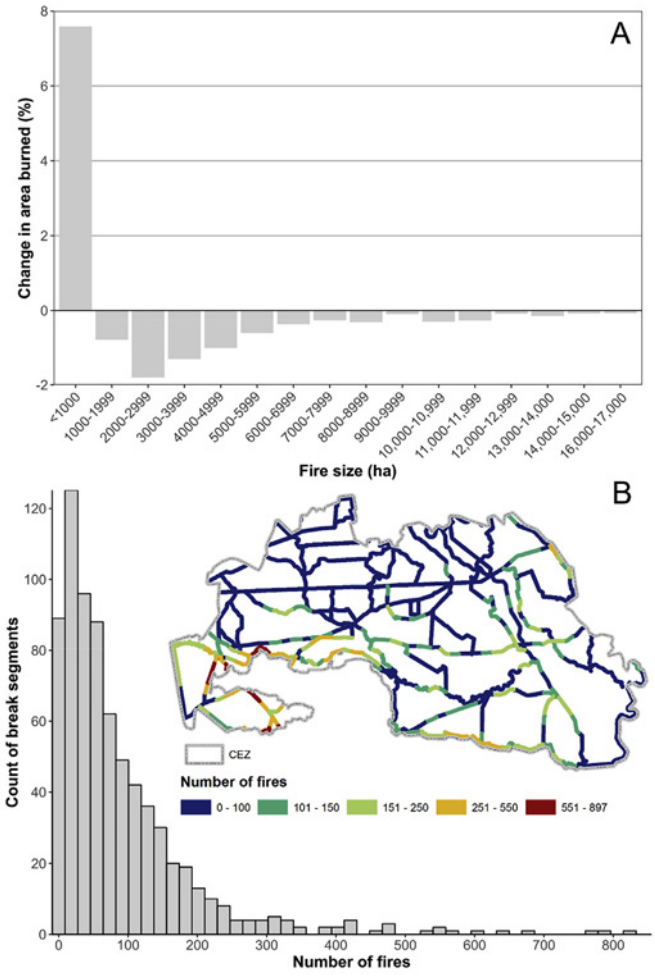

Fig. 7. A) Change in fire size distribution with fuel breaks as implemented in Fig. 6 within the Chernobyl Exclusion Zone (CEZ). Graph shows that fuel breaks increase the number of small fires while reducing larger fire events. B) Intercept frequency and spatial location of simulated fires and fuel break segments for the treated landscape in the CEZ. Fuel breaks were discretized into 2 km segments and the number of encounters with wildfires were recorded for the individual scenarios.

emissions (Fig. 8) within the CEZ showed the highest reduction in areas around the power plant (near Prypiat) and the southwest portion of the CEZ where ignitions are relatively common. There were only minor differences between the expected and potential emissions, the former considering ignition probability, while the latter is the effect of the fuel breaks conditional on a fire ocurring.

4. Discussion

4.1. Summary of results

Fine-scale wildfire simulation modeling was employed to examine potential wildfire-caused ^{137}Cs emissions in the areas contaminated by the Chernobyl nuclear disaster. The outputs from the simulation modeling are consistent with historical data on fire frequency, intensity, and behavior (Zibtsev et al., 2011). The simulation outputs augment the sparse historic record of large wildfire events to provide a set of predictive and finer-scale maps of risk components absent in prior coarse-scale studies (Evangeliou et al., 2015; Hohl et al., 2012). Specifically, prior assessment of fire hazard in the CEZ, as reported in Zibtsev et al. (2015), includes five hazard classes and does not consider post-fire contamination, lacks any quantitative assessment of fire behavior or wildfire likelihood, and assumes an even space-time distribution of ignitions. Moreover, it is commonly assumed that fire risk is higher in the summer (Evangeliou et al., 2015) when, in fact, human activities associated with field burning occur in the spring and fall, thus significantly influencing the temporal pattern of risk. The modeling outputs described here provide plausible future fire event scenarios and the relative amounts of ^{137}Cs resuspension from these events, in contrast to previous coarse-scale studies that estimated radionuclide emissions under the assumption that major portions of the CEZ burned (Evangeliou et al., 2014; Hohl et al., 2012).

One broad limitation of our study is that we only considered effects of wildfire on resuspension of ^{137}Cs. Contamination by ^{238,239,240}Pu, ^{90}Sr or ^{241}Am were not assessed. While the spatial distribution of these latter radionuclides is similar to ^{137}Cs (Appendix A, Fig. A6), the one significant difference is the existence of a ^{137}Cs specific deposition plume oriented to the southwest that probably occurred on April 26 (Kashparov et al., 2016; Fig. 1.4). However, resuspension from wildfire in relation to fire severity is significantly different among the radionuclides, owing to different soil migration patterns among the radionuclides and variation in the soils themselves.

Our analysis revealed a number of hotspots in terms of both fire likelihood and intensity and identified locations where ignitions can potentially result in large fires that contribute to radionuclide emissions (Fig. 5B). These hotspots resulted from areas with high historical probability of ignitions, primarily in grasslands with high fire spread rates that spread into conifer plantations that are highly susceptible to crown fire. While grassland fuels have relatively low fire hazard potential, the rapid spread rate and potential to spread into forest fuels as large spreading fronts results in a difficult suppression problem.

Our emissions potential map (Fig. 5A) shows the potential of each ignition location to generate a fire and resuspend radionuclides. This map can be overlayed on maps of suppression difficulty, firefighting response time, fuels composition (forest versus grass), and existing fuel breaks to identify where existing wildfire management practices can be refined and targeted to reflect potential emissions at specific ignition locations. Our analysis allows identification of the source of risk, an additional dimension of risk (Gardoni and Murphy, 2014) that should be factored into risk evaluation, yet is not done in most wildfire risk assessments. We did not attempt to develop quantitative response functions that explicitly linked fire intensity with emissions, owing to large uncertainty in the literature on emissions factors (see Section 2.4), but rather use the outputs to examine spatial variation in potential emissions assuming an emissions factor of 0.05.

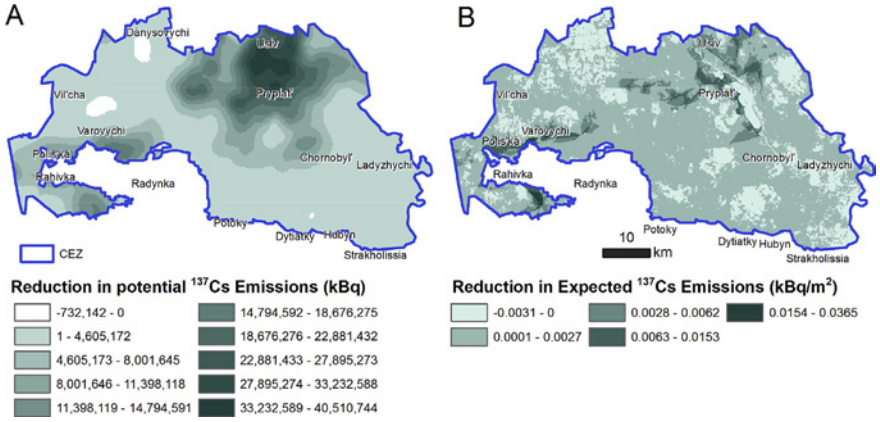

Fig. 8. Change in potential (A) and expected emissions (B) from a fuel break network as implemented in Fig. 6 in the Chernobyl Exclusion Zone (CEZ). For the untreated and treated (fuel break) landscapes each simulated ignition point was colored according to the total 2018 ^{137}Cesium (Cs) contamination potentially resuspended within the resulting fire perimeter. The smoothed map was then differenced to show the net reduction from the fuel breaks as either the potential (given an ignition, A), and the expected value corrected for the ignition probability.

Our study is also the first to examine the drivers of wildfire events and juxtaposition of wildfires and contaminated areas within both Belarus and Ukraine. The model outputs show that while the potential for wildfire-caused radionuclide emissions is significant in the PER in terms of fire size, intensity, and levels of contamination, the predicted wildfire activity is quite low, as a result of low ignition frequency (Fig. 4A) due to security measures taken within the contaminated areas.

4.2. Identifying the drivers of fire in contaminated areas

The future trajectory of burned area over time within the CEZ and PER is a complex question with multiple drivers of fire ignition, spread, and intensity, and future climate all affecting radionuclide resuspension from wildfires. The question of the relative importance of these drivers deserves close scrutiny in the design of mitigation systems. Although climatic anomalies were largely responsible for the recent large fires in the CEZ, as elsewhere in Australia (Cruz et al., 2012) and the Mediterranean region, high intensity crown fire from fuel buildup in forests compromised suppression efforts. Zibtsev et al. (2015) state that the fuels buildup from the lack of forest management is the primary driver of such conditions. Evangeliou et al. (2015) further argue that based on relationships between forested area and burned area in central Europe, succession of former agricultural areas into forests within the CEZ could reduce fragmentation in forest fuels and lead to increased burned area. However, there are several issues with downscaling fire regimes in central Europe to the CEZ and PER, including the fact that under all but extreme weather conditions, grass and shrub fuels have higher rates of spread (Scott and Burgan, 2005) that result in higher burn probabilities in fire prone areas. Globally, grass fires are naturally larger, faster spreading, and account for the bulk of the annual area burned. While it is true that high intensity forest fires are often more difficult to control, the higher spread rates of grassland fires can contribute to a lower success rate on initial attack, and grassland patches can accelerate fire into large forested areas. Fire spread is also strongly affected by factors other than forest-grassland ratios including the shape, size, and arrangement of the respective fuel patches (Finney, 2001). Seasonal weather also effects the relative spread rates of forests versus grasslands since in both the CEZ and PER, forest fuels have relatively high fuel moistures in the spring and are not susceptible to burning, while grasslands and crop residues have relatively low fuel moisture and are highly flammable.

While the buildup in forest fuels contributed to increasing area burned in the last decade, the potential for large fires is largely driven by human activities both outside and inside the CEZ that result in fire ignitions. While the increased fuels caused by lack of management contribute to reduced suppression effectiveness, increased fire severity, and larger fires, the potential to mitigate this through ignition prevention is clearly shown in the historical ignition data within the Polesie reserve (Figs. 3B and 4A). Improved security to reduce unauthorized access to the PER was instituted in 1991 to address the wildfire problem that resulted in a dramatic drop in ignitions (Figs. 3B and 4A), burn probablity (Fig. 4C), and risk of resuspension (Fig. 5B). The vast bulk of the ignitions and area burned within the CEZ and PER was caused by activities related to burning of crop residue and weeds, industrial activities, and arson (Dancause et al., 2010; Zibtsev et al., 2015). The 9241-ha fire in April 2015, for instance, started as a field burn by local villagers, persisted as a peat fire over the winter, and then re-ignited in the spring within a dry grassland and spread to the CEZ. A number of recent fires including one near the reactor in 2017 was either intentionally set or resulted from negligence (e.g., cigarette smoking) (personal communication). Illegal and unmonitored re-settlement within the CEZ are contributing to more ignitions related to farm activities. This contradicts the assessment of Evangeliou et al. (2015; pg. 61), which states that, "most fires in these areas were attributable to natural causes such as lightning." However, historical databases list confirmed lightning fires in only 4 years of the 17-year record and amounted to 2.75% of the total ignitions with an average size of 7.5-ha. Moreover, the spatial patterns of ignitions are clearly correlated with human activities.

4.3. The potential for risk transmission from wildfires

The April 2015 wildfire in the CEZ and additional fires in the Polesie reserve (ca. 10,000 ha) and in other contaminated areas redistributed radionuclides over the northern and eastern parts of Europe, and an August wildfire (5698 ha) affected Central and Southern Europe. These releases of radionuclides by wildfire smoke were classified as Level 3 on the INES (International Nuclear Events Scale) that corresponds to a serious incident, in which non-lethal deterministic effects are expected (Evangeliou et al., 2015; IAEA, 2013). Experimental burning of vegetation within the CEZ under marginal, moist, burning conditions, concluded that these small experimental fires impacted a relatively small area downwind and that the contribution of such fires to the redistribution of radioactivity in and outside the CEZ would be negligible (Yoschenko et al., 2006). Prior investigations of potential wildfire ^{137}Cs emissions have presented dramatically different scenarios and emissions estimates, but meaningful comparisons with our study are difficult. Evangeliou et al. (2014) analyzed wildfire scenarios that assumed burning of 10%, 50%, and 100% of the contaminated forests in Russia, Belarus, and Ukraine, but the specific forests are not identified in terms of contamination levels. The emissions from the 10% estimate was 0.29 PBq, whereas randomly burning 10% of our study area that captures the bulk of the contaminated area, yields an estimate of

Table 1
Wildland fire system components and key recommendations for enhancing short- and long-term risk management within the Chernobyl Exclusion Zone (CEZ).

Wildland fire system component	Recommendations[a]
Wildland fire ignition prevention	• Initiate public and industrial ignition prevention programs (Prestemon et al., 2010) • Improve border security to reduce unauthorized access to the CEZ (Ager et al., 2015) • Training for industrial workers (gas pipeline/-electrical network, foresters, road construction, drivers engaged) in practices to reduce fire ignitions • Restrict all agricultural burning within the CEZ • Establish and enforce regulations to reduce wildfires from agricultural burning outside the CEZ within a 10 km buffer
Initial attack and extended suppression	• Build a wildland fire decision support system (Noonan-Wright et al., 2011) • Adopt an Incident Command System (ICS) to provide effective management and coordination of firefighting resources for initial attack and extended duration wildfire events (Lasko, 2011) • Reexamine procedures for firefighter operations in radioactively contaminated environments and establish protocols for firefighter exposure monitoring (Lasko, 2011) • Implement a system of fire detection and meteorological observation sites to provide continuous wildfire detection and meteorological monitoring • Acquire dependable helicopter capability to enable rapid, surveillance, assessment, and suppression of wildfires (Lasko, 2011) • Map water sources for aerial and ground suppression resources • Build a suppression transportation routing system to minimize response time to wildfire ignitions (Zibtsev et al., 2015) • Institute a protocol that dedicates all CEZ field and fire staff to wildfire initial attack when fire weather danger exceeds class IV and wind speed is >6 m/s
Fuels management	• Assess wildfire risk and potential to develop and prioritize fuels management activities (Hao et al., 2009; Lasko, 2011; Usenia et al., 2017) • Establish a network of firebreaks (Oliveira et al., 2016; Syphard et al., 2011) • Develop a strategy for managing harvested, radioactive wood (e.g., incineration, solidification, or long-term storage and sequestration) • Expand research into strategic restoration of hardwood forests and develop landscape management plan to reduce potential for large crown fire events
Strategic management and risk governance	• Continue to develop and integrate fire prevention, detection, fire suppression, and fuels management actions into an operational and comprehensive fire management plan (Zibtsev et al., 2015) • Develop and incorporate GIS layers (e.g., fire hazard, forest conditions, radioactive contamination, transportation systems, fire break locations, energy transmission networks, fire history, water sources, and wildfire response facilities) into the CEZ fire management plan (Hao et al., 2009; Lasko, 2011) • Translate remote sensing technology, fuels management, fire behavior assessment, wildfire suppression, and incident command system reference material into Ukrainian to facilitate technology transfer to Ukrainian fire managers (Hao et al., 2009; Lasko, 2011) • Integrate wildland fire mitigation planning with Biosphere management planning (Government of Ukraine, 2019); continue cooperation and coordination of fire management activities with Polesie Radioecological Reserve • Reexamine and update firefighting tactics, protective equipment, and fire personnel training to safely fight wildfires in radioactively contaminated environments (Lasko, 2016) • Reexamine and update protocols for monitoring firefighter exposure to radioactive contamination (Lasko, 2016) • Build institutional system for coordinating and integrating firefighting management and operations for CEZ wildfire response personnel

[a] Recommendations are a synthesis of Zibtsev et al. (2015), Lasko (2011); Lasko (2016), Hao et al. (2009), and the authors of the current study.

0.0014 or 200 times less than Evangeliou et al. (2014). Note that 10% of our study area could be burned in wildfires without significant emissions considering the extreme spatial variability in ^{137}Cs deposition (Fig. 1), and that much of the forests in the contaminated areas are deciduous forests in bogs and wetlands with high fuel moistures, protected by waterways and rivers, and unlikely to burn at high intensity if at all under any known weather scenario. In a more recent study of actual wildfire events, Evangeliou et al. (2015) combined satellite images of real fires in 2002, 2008, and 2010 with measurements of radioactive ^{137}Cs deposited on the area, and models of air movements and fires. They estimated that these wildfires have cumulatively redistributed over Europe an estimated 8% of the original amount of ^{137}Cs released in the 1986 disaster. Specifically, they estimated that of the 85 PBq of ^{137}Cs released by the Chernobyl accident, between 2 and 8 PBq are still contained in the upper layer of soil in the exclusion zone. The three fires released 2–8% of the ^{137}Cs (assuming for the entire incident not just Chernobyl), and some 0.5 PBq in smoke. This was distributed over Eastern Europe and detected as far south as Turkey, and as far west as Italy and Scandinavia.

4.4. Fuel breaks

Our modeling system is particularly well suited for designing and testing alternative fuel break networks to quantitate performance in terms of encounter rate, fire size distribution and avoided emissions. Although optimal protection from the fuel breaks was assumed, meaning they were rarely breached by the simulated fires, this is a best-case scenario, and results are still useful to communicate the utility of fuel break systems to national and international audiences, and can be used for strategic planning to improve existing fuel break systems. The CEZ forest management plan called for 111.9 km of fuel breaks of variable dimensions, most >20-m wide, primarily along external perimeters and roads. They are essentially no longer maintained, and no digital map exists of either the originally planned fuel breaks or a strategic plan to build them (Zibtsev et al., 2015). This is in contrast to the well-maintained fuel break network in the PER maintained by fire management organizations (Appendix A, Fig. A3B). Forest management has not been implemented in the CEZ due to lack of funding and only 50% of planned thinning was carried out between 2004 and 2006, despite the fact that extensive areas have low contamination (45%) and management is allowed. Fuel breaks could be strategically designed in the CEZ to use natural breaks along streams and marshes, and boundaries along former farm fields to improve suppression effectiveness while considering the potential for large fire spread into contaminated areas. Prioritization of fuel breaks can be accomplished by mapping of contamination levels along all the roads to find the road segments that are most effective at blocking fire spread from non-contaminated to highly contaminated areas. The network could also be expanded outside of the CEZ to lower the risk of incoming fires from ignition hotspots immediately outside the zone. New technologies would facilitate the creation and maintenance of fuel breaks through forested areas, including high capacity chipping machines and nuclear waste solidification capacity.

Future application of the model can be refined to consider localized conditions with respect to crown fire and spotting. In this way the most vulnerable fuel break segments can be identified.

4.5. The future of fire management in contaminated areas

The spatial patterns in risk factors identified in this study and prior reports by USDA Forest Service fire managers (Lasko, 2011; Lasko, 2016) and Ukrainian scientists (Zibtsev et al., 2015) can help managers and policymakers develop a comprehensive fire management strategy. USDA Forest Service specialists are now combining these various layers to create a zonal strategy map to prioritize various integrated mitigation actions. For example, information on travel time (Zibtsev et al., 2015), ignition potential (Fig. 4A), and contamination (Fig. 5) reveal where road access needs to be improved for prevention patrolling, fire infrastructure maintenance and initial attack. In this way effective management of fire risk and radionuclide re-suspension within the contaminated areas can take a multifaceted approach as developed in the US cohesive fire management strategy (USDA-USDI, 2013). Here, ignition prevention, detection, initial attack, suppression, and fuel management investments designed to manage wildfire risk are space-time optimized and spatially allocated as determined from modeling exercises like that conducted in this study. Although there is some progress toward this type of analysis (Zibtsev et al., 2015), and many policy documents to support it (Hao et al., 2009; Lasko, 2016), prior work has lacked landscape fire behavior information like that generated in the current study and failed to consider integrating fuel breaks with other fire management activities. In the long run, leveraging fire management science to build a multifaceted fire management plan will need a well-organized risk governance system. Response to wildfire events in the CEZ is bifurcated with two agencies: the State Specialized Forestry Enterprise Pivnichna Puscha (Ministry of Ecology and Natural Resources - State Agency for Exclusion Zone Management) and the Department of Emergency Response (State Emergency Service of Ukraine). The future of wildfire management is further complicated by the newly formed Biosphere Reserve (Government of Ukraine, 2019) that establishes a zone of waste management (10-km surrounding the reactor site) with the remaining area in one of three zones (core protected, buffer to the core, and anthropogenic activities). The zones permit increasing levels of management intensity, ranging from the total prohibition of management activities in the protected zone to intensive forest management activities in the anthropogenic zone. The impact of the Biosphere Reserve on fire management is uncertain at this time. Although fire suppression activities are expected to be allowed in all zones, fuel break construction, road building, and vegetation modification projects would be limited to zones allowing anthropogenic management. The probability of human caused ignitions might decrease in the core nature reserve and buffer zones if human access is strictly controlled but may increase in controlled regime and anthropogenic zones where access and industrial forest operations are expected to increase.

Finally, to bridge our work with prior wildfire research and policy discussions concerning wildfires in contaminated areas (Hao et al., 2009; Lasko, 2011; Zibtsev et al., 2015) we created a comprehensive set of key recommendations (Table 1) for the development of a strategic wildfire management plan for the CEZ. These recommendations should be implemented with the understanding that under projected changes in climate, drought-induced fires will increasingly challenge fire management programs and resuspended radionuclides will potentially create adverse health consequences to the affected population and environment.

Declaration of Competing Interest

The authors declare that they have no known competing financial interests or personal relationships that could have appeared to influence the work reported in this paper.

Acknowledgements

This work was partially funded by the USDA Forest Service International Programs. We thank Shelia Slemp, Forest Service International Programs, for past and continued support of the wildfire management and research mission in Ukraine. We are also grateful to Ken Bunzel and Chris Ringo for support on spatial analysis. We thank Matt Gregory for a review of the fuels data methodology and three anonymous reviewers.

Appendix A. Supplementary data

Supplementary data to this article can be found online at https://doi.org/10.1016/j.scitotenv.2019.133954.

References

Ager, A.A., Finney, M.A., Lasko, R.J., Evers, C., 2015. Probabilistic Wildfire and Fuels Risk Assessment for the Chernobyl Exclusion Zone. USDA Forest Service, Washington, D.C.
Ager, A.A., Barros, A., Day, M.A., Preisler, H.K., Spies, T., Bolte, J., 2018. Analyzing fine-scale spatiotemporal drivers of wildfire in a forest landscape model. Ecol. Model. 384, 89–102.
Alcasena, F.J., Salis, M., Vega-García, C., 2016. A fire modeling approach to assess wildfire exposure of valued resources in central Navarra, Spain. Eur. J. For. Res. 135, 87–107.
Amiro, B., Sheppard, S., Johnston, F., Evenden, W., Harris, D., 1996. Burning radionuclide question: what happens to iodine, cesium and chlorine in biomass fires? Sci. Total Environ. 187, 93–103.
Amiro, B.D., Dvornik, A.T., Zhuchenko, T., 1999. Fire and radioactivity in contaminated forests. In: Linkov, I., Schell, W.R. (Eds.), Contaminated Forests. Kluwer Academic Publishers, Dordrecht, pp. 311–324.
Avramenko, T.V., Veremeeva, A.A., Zhukova, O.M., Kompanets, L.V., Kruglov, S.A., Makarova, O.A., et al., 2009. Atlas of Modern and Predicted Aspects of Consequences of the Accident at Chernobyl NPP in the Affected Territories of Russian and Belarus. Infosfera Foundation, Minsk.
Baig, M.H.A., Zhang, L., Shuai, T., Tong, Q., 2014. Derivation of a tasselled cap transformation based on Landsat 8 at-satellite reflectance. Remote Sensing Letters 5, 423–431.
Bey, A., Sánchez-Paus Díaz, A., Maniatis, D., Marchi, G., Mollicone, D., Ricci, S., et al., 2016. Collect earth: land use and land cover assessment through augmented visual interpretation. Remote Sens. 8, 807.
Bogorad, V.I., Litvinskaya, T.V., Shevchenko, I.A., Dybach, A.M., Slepchenko, A.Y., 2016. Radiation consequences of fire in Chornobyl NPP exclusive zone. Nuclear and Radiation Safety 1.
Breiman, L., 2001. Random forests. Mach. Learn. 45, 5–32.
Brittain, S., 2017. Fire Behavior Applications and Libraries. Alturas Solutions, Missoula, MT.
Brown, J.E., Bondar, Y., Kashparov, V., Nalbandyan, A., Navumav, A., Skipperud, L., et al., 2011. Radioactive contamination in the Belarusian sector of the Chernobyl exclusion zone. Radioprotection 46, S771–S777.
Burger, A., Lichtscheidl, I., 2018. Stable and radioactive cesium: a review about distribution in the environment, uptake and translocation in plants, plant reactions and plants' potential for bioremediation. Sci. Total Environ. 618, 1459–1485.
Chakrabarty, R.K., Moosmüller, H., Garro, M.A., Arnott, W.P., Walker, J., Susott, R.A., et al., 2006. Emissions from the laboratory combustion of wildland fuels: particle morphology and size. J. Geophys. Res. 111, 1–16.
Cruz, M.G., Sullivan, A.L., Gould, J.S., Sims, N.C., Bannister, A.J., Hollis, J.J., et al., 2012. Anatomy of a catastrophic wildfire: the Black Saturday Kilmore East fire in Victoria, Australia. For. Ecol. Manag. 284, 269–285.
Dancause, K.N., Yevtushok, L., Lapchenko, S., Shumlyansky, I., Shevchenko, G., Wertelecki, W., et al., 2010. Chronic radiation exposure in the Rivne-Polissia region of Ukraine: implications for birth defects. Am. J. Hum. Biol. 22, 667–674.
Davoine, X., Bocquet, M., 2007. Inverse modelling-based reconstruction of the Chernobyl source term available for long-range transport. Atmos. Chem. Phys. 7, 1549–1564.
De Cort, G., Dubois, G., Fridman, S.D., Germenchuk, M.G., Izrael, Y.A., Janssens, A., et al., 1998. Atlas of Caesium Deposition on Europe After the Chernobyl Accident, Luxembourg.
Dixon, G.E., Keyser, C.E., 2008. Lake States (LS) Variant Overview – Forest Vegetation Simulator. Internal Rep. USDA Forest Service, Forest Management Service Center, Fort Collins, CO.
Dvornik, A., Klementeva, E., Dvornik, A., 2017. Assessment of ^{137}Cs contamination of combustion products and air pollution during the forest fires in zones of radioactive contamination. Radioprotection 52, 29–36.
Evangeliou, N., Balkanski, Y., Cozic, A., Hao, W.M., Møller, A.P., 2014. Wildfires in Chernobyl-contaminated forests and risks to the population and the environment: a new nuclear disaster about to happen? Environ. Int. 73, 346–358.
Evangeliou, N., Balkanski, Y., Cozic, A., Hao, W.M., Mouillot, F., Thonicke, K., et al., 2015. Fire evolution in the radioactive forests of Ukraine and Belarus: future risks for the population and the environment. Ecol. Monogr. 85, 49–72.
Evangeliou, N., Zibtsev, S., Myroniuk, V., Zhurba, M., Hamburger, T., Stohl, A., et al., 2016. Resuspension and atmospheric transport of radionuclides due to wildfires near the Chernobyl nuclear power plant in 2015: an impact assessment. Sci. Rep. 6, 26062.
Finney, M.A., 2001. Design of regular landscape fuel treatment patterns for modifying fire growth and behavior. For. Sci. 47, 219–228.

Finney, M.A., 2002. Fire growth using minimum travel time methods. Can. J. For. Res. 32, 1420–1424.
Finney, M.A., McHugh, C.W., Grenfell, I.C., Riley, K.L., Short, K.C., 2011. A simulation of probabilistic wildfire risk components for the continental United States. Stoch. Env. Res. Risk A. 25, 973–1000.
Gardoni, P., Murphy, C., 2014. A scale of risk. Risk Anal. 34, 1208–1227.
Gorelick, N., Hancher, M., Dixon, M., Ilyushchenko, S., Thau, D., Moore, R., 2017. Google earth engine: planetary-scale geospatial analysis for everyone. Remote Sens. Environ. 202, 18–27.
Government of Ukraine, 2019. Chornobyl Radiation and Ecological Biosphere Reserve. http://zapovidnyk.org.ua/.
Hansen, M.C., Stehman, S.V., Potapov, P.V., 2010. Quantification of global gross forest cover loss. Proc. Natl. Acad. Sci. 107, 8650–8655.
Hansen, M.C., Potapov, P.V., Moore, R., Hancher, M., Turubanova, S., Tyukavina, A., et al., 2013. High-resolution global maps of 21st-century forest cover change. Science 342, 850–853.
Hansen, M., Egorov, A., Potapov, P., Stehman, S., Tyukavina, A., Turubanova, S., et al., 2014. Monitoring conterminous United States (CONUS) land cover change with web-enabled Landsat data (WELD). Remote Sens. Environ. 140, 466–484.
Hao, W., Bondarenko, O.O., Zibtsev, S., Hutton, D., 2009. Chapter 12 vegetation fires, smoke emissions, and dispersion of radionuclides in the Chernobyl exclusion zone. In: Bytnerowicz, A., Arbaugh, M., Riebau, A., Andersen, C. (Eds.), Developments in Environmental Science, Volume 8: Wildland Fires and Air Pollution. Elsevier, The Netherlands, pp. 265–275.
Hao, W.M., Baker, S., Lincoln, E., Hudson, S., Lee, S.D., Lemieux, P., 2018. Cesium emissions from laboratory fires. J. Air Waste Manage. Assoc. 68, 1211–1223.
Hohl, A., Niccolai, A., Oliver, C., Melnychuk, D., Zibtsev, S., Goldammer, J.G., et al., 2012. The human health effects of radioactive smoke from a catastrophic wildfire in the Chernobyl exclusion zone: a worst case scenario. Earth Bioresources and Quality of Life 1, 1–34.
Horrill, A., Kennedy, V., Paterson, I., McGowan, G., 1995. The effect of heather burning on the transfer of radiocaesium to smoke and the solubility of radiocaesium associated with different types of heather ash. J. Environ. Radioact. 29, 1–10.
IAEA, 2006. Environmental consequences of the Chernobyl accident and their remediation: Twenty years of experience. Report of the Chernobyl Forum Expert Group "Environment". International Atomic Energy Agency, Vienna, Austria.
IAEA, 2013. INES: The International Nuclear and Radiological Event Scale. 2008 edition. International Atomic Energy Agency, Vienna.
Kashparov, V.A., Lundin, S.M., Kadygrib, A.M., Protsak, V.P., Levtchuk, S.E., Yoschenko, V.I., et al., 2000. Forest fires in the territory contaminated as a result of the Chernobyl accident: radioactive aerosol resuspension and exposure of fire-fighters. J. Environ. Radioact. 51, 281–298.
Kashparov, V., Lundin, S., Khomutinin, Y.V., Kaminsky, S., Levchuk, S., Protsak, V., et al., 2001. Soil contamination with ^{90}Sr in the near zone of the Chernobyl accident. J. Environ. Radioact. 56, 285–298.
Kashparov, V., Zhurba, M., Zibtsev, S., Mironyuk, V., Kireev, S., 2015. Evaluation of the expected doses of fire brigades at the Chornobyl exclusion zone in April 2015. Yaderna Fyizika ta Energetika 16, 399–407.
Kashparov, V., Levchuk, S., Khomutynyn, I., Morozova, V., Zhurba, M., 2016. Chernobyl: 30 years of radioactive contamination legacy. Earth System Science Data. Ukrainian Institute of Agricultural Radiology of National University of Life and Environmental Sciences of Ukraine, Kiev, Ukraine.
Kashparov, V., Levchuk, S., Zhurba, M., Protsak, V., Khomutinin, Y., Beresford, N.A., et al., 2018. Spatial datasets of radionuclide contamination in the Ukrainian Chernobyl exclusion zone. Earth System Science Data 10, 339–353.
Kovalets, I.V., Romanenko, A.N., Anulich, S.N., Ievdin, I.A., 2015. Forecasting of the radioactive contamination by Cs-137 following fires in Chernobyl exclusion zone in April-May, 2015. Proceedings of the Decision Support Systems, Theory and Practice Conference, Kiev, Ukraine.
Kudin, M.V., 2014. Burnability of forest of Belorussian and Ukrainian sectors of the exclusion zone of cherboyl nuclear power plant. Scientific Bulletin of the Institute of Forest of the National Academy of Sciences of Belarus. vol. 74, pp. 530–551.
Lasko, R., 2011. Assessment and Potential Management Actions to Mitigate Effects of Forest and Grassland Fires in Chornobyl Exclusion Zone. USDA Forest Service, Washington DC, p. 16.
Lasko, R., 2016. Mitigating the Effects of Wildfire in the Chernobyl Exclusion Zone. USDA Forest Service, Washington DC.
Miller, C., Ager, A.A., 2013. A review of recent advances in risk analysis for wildfire management. Int. J. Wildland Fire 22 (1), 14.
Møller, A.P., Barnier, F., Mousseau, T.A., 2012. Ecosystems effects 25 years after Chernobyl: pollinators, fruit set and recruitment. Oecologia 170, 1155–1165.
NASA, 2015. MODIS Collection 6 NRT Hotspot/Active Fire Detections MCD14DL. NASA Land Processes Distributed Active Archive Center (LP DAAC).
Nelson, R.M., 2000. Prediction of diurnal change in 10-h fuel stick moisture content. Can. J. For. Res. 30, 1071–1087.
Noonan-Wright, E.K., Opperman, T.S., Finney, M.A., Zimmerman, G.T., Seli, R.C., Elenz, L.M., et al., 2011. Developing the US wildland fire decision support system. J. Comb. 168473, 14.
Oliveira, T.M., Barros, A.M.G., Ager, A.A., Fernandes, P.M., 2016. Assessing the effect of a fuel break network to reduce burnt area and wildfire risk transmission. Int. J. Wildland Fire 25, 619–632.
Olofsson, P., Foody, G.M., Herold, M., Stehman, S.V., Woodcock, C.E., Wulder, M.A., 2014. Good practices for estimating area and assessing accuracy of land change. Remote Sens. Environ. 148, 42–57.
Palaiologou, P., Ager, A.A., Nielsen-Pincus, M., Evers, C., Kalabokidis, K., 2018. Using transboundary wildfire exposure assessments to improve fire management programs: a case study in Greece. Int. J. Wildland Fire 27, 501–513.
Paller, M.H., Jannik, G., Baker, R., 2014. Effective half-life of caesium-137 in various environmental media at the Savannah River site. J. Environ. Radioact. 131, 81–88.
Pazukhin, E.M., Borovoi, A.A., Ogorodnikov, B.I., 2004. Forest fire as a factor of environmental redistribution of radionuclides originating from Chernobyl accident. Radiochemistry 46, 102–106.
Prestemon, J.P., Butry, D.T., Abt, K.L., Sutphen, R., 2010. Net benefits of wildfire prevention education efforts. For. Sci. 56, 181–192.
Salis, M., Ager, A., Arca, B., Finney, M.A., Bacciu, V., Duce, P., et al., 2013. Assessing exposure of human and ecological values to wildfire in Sardinia, Italy. Int. J. Wildland Fire 22, 549–565.
Scott, J.H., Burgan, R.E., 2005. Standard Fire Behavior Fuel Models: A Comprehensive Set for Use With Rothermel's Surface Fire Spread Model. USDA Forest Service, Rocky Mountain Research Station, Fort Collins, CO, p. 72.
Shcheglov, A., Og, Tsvetnova, Klyashtorin, A., 2014. Biogeochemical cycles of Chernobyl-born radionuclides in the contaminated forest ecosystems. Long-term dynamics of the migration processes. J. Geochem. Explor. 144, 260–266.
SNRIU, 2019. Modeling the Atmospheric Transport of Combustion Products as a Result of a Forest Fire in the Chernobyl Exclusion Zone Indicates the Absence of Exceeding the Normative Values of the Concentration of Radionuclides. State Nuclear Regulatory Inspectorate of Ukraine.
State Special Enterprise Picnichna Puscha, 2019. Fire Statistics in the Forest Lands in the Exclusion Zone, Chornobyl, Ukraine.
Syphard, A.D., Keeley, J.E., Brennan, T.J., 2011. Factors affecting fuel break effectiveness in the control of large fires on the Los Padres National Forest, California. Int. J. Wildland Fire 20, 764–775.
Talerko, N., 2005. Mesoscale modelling of radioactive contamination formation in Ukraine caused by the Chernobyl accident. J. Environ. Radioact. 78, 311–329.
Talerko, M.M., 2011. Reconstruction and Prognosis of Radioactive Contamination as a Result of Communal Radiation Accident Using Atmospheric Transport Modeling (With Example of Chornobyl Accident). Dissertation. National Academy of Science of Ukraine, Kyiv, Ukraine.
Talerko, M., Garger, E., Kuzmenko, A.G., 2010. A computer system for assessment and forecasting of radiation situation in the Chernobyl exclusion zone. Nuclear and Radiation Safety 47, 45–59.
Ukrainian Hydrometeorological Center, 2016. Meteorological Station of Chornobyl City.
USDA-USDI, 2013. A National Cohesive Wildland Fire Management Strategy: Challenges, Opportunities, and National Priorities. United States Department of Agriculture-United States Department of Interior, p. 104.
Usenia, V.V., 2002. Forest Fires, Impacts and Suppression. Gomel, Belarus. .
Usenia, V.V., Yurievich, N.N., 2017. The experience of Belarus in forest fire suppression. Sustainable Forest Management 2, 14–21.
Usenia, V.V., Gordey, N.V., Katkova, E.N., 2017. Improving forest fire risk zoning of the territory of Belarus. Proceedings of Belarusian State Technological University Forestry Series: Environmental Management. Reprocessing of Renewable Resources vol. 2, pp. 115–121.
Whicker, F.W., Schultz, V., 1982. Radioecology: Nuclear Energy and the Environment. Vol. 2. CRC press, Boca Raton, FL.
Yablokov, A.V., Nesterenko, A.V., Nesterenko, V.B., Sherman-Nevinger, J.D., 2009. Chernobyl: Consequences of the Catastrophe for People and the Environment. Vol. 1181. New York Academy of Sciences, New York.
Yoschenko, V.I., Kashparov, V.A., Levchuk, S.E., Glukhovskiy, A.S., Khomutinin, Y.V., Protsak, V.P., et al., 2006. Resuspension and redistribution of radionuclides during grassland and forest fires in the Chernobyl exclusion zone: part II. Modeling the transport process. J. Environ. Radioact. 87, 260–278.
Zibtsev, S., Oliver, C., Goldammer, J., Hohl, A., McCarter, J., Niccolai, A., et al., 2011. Wildfires risk reduction from forests contaminated by radionuclides: a case study of the Chernobyl nuclear power plant exclusion zone. International Wildland Fire Conference, Sun City, South Africa, p. 23.
Zibtsev, S., Goldammer, J., Robinson, S., Borsuk, O., 2015. Fires in nuclear forests: silent threats to the environment and human security. Unasylva 66, 40–51.